



Kent Academic Repository

Lean, Fabian Z. X., Lamers, Mart M., Smith, Samuel P., Shipley, Rebecca, Schipper, Debby, Temperton, Nigel J., Haagmans, Bart L., Banyard, Ashley C., Bewley, Kevin R., Carroll, Miles W. and others (2020) *Development of immunohistochemistry and in situ hybridisation for the detection of SARS-CoV and SARS-CoV-2 in formalin-fixed paraffin-embedded specimens*. *Scientific Reports*, 10 (1). pp. 1-9. ISSN 2045-2322.

Downloaded from

<https://kar.kent.ac.uk/84817/> The University of Kent's Academic Repository KAR

The version of record is available from

<https://doi.org/10.1038/s41598-020-78949-0>

This document version

Publisher pdf

DOI for this version

Licence for this version

UNSPECIFIED

Additional information

Versions of research works

Versions of Record

If this version is the version of record, it is the same as the published version available on the publisher's web site. Cite as the published version.

Author Accepted Manuscripts

If this document is identified as the Author Accepted Manuscript it is the version after peer review but before type setting, copy editing or publisher branding. Cite as Surname, Initial. (Year) 'Title of article'. To be published in *Title of Journal*, Volume and issue numbers [peer-reviewed accepted version]. Available at: DOI or URL (Accessed: date).

Enquiries

If you have questions about this document contact ResearchSupport@kent.ac.uk. Please include the URL of the record in KAR. If you believe that your, or a third party's rights have been compromised through this document please see our [Take Down policy](https://www.kent.ac.uk/guides/kar-the-kent-academic-repository#policies) (available from <https://www.kent.ac.uk/guides/kar-the-kent-academic-repository#policies>).



OPEN

Development of immunohistochemistry and in situ hybridisation for the detection of SARS-CoV and SARS-CoV-2 in formalin-fixed paraffin-embedded specimens

Fabian Z. X. Lean¹✉, Mart M. Lamers², Samuel P. Smith^{3,7}, Rebecca Shipley^{3,6}, Debby Schipper², Nigel Temperton⁴, Bart L. Haagmans², Ashley C. Banyard³, Kevin R. Bewley⁵, Miles W. Carroll⁵, Sharon M. Brookes³, Ian Brown³ & Alejandro Nuñez¹

The rapid emergence of SARS-CoV-2, the causative agent of COVID-19, and its dissemination globally has caused an unprecedented strain on public health. Animal models are urgently being developed for SARS-CoV-2 to aid rational design of vaccines and therapeutics. Immunohistochemistry and in situ hybridisation techniques that facilitate reliable and reproducible detection of SARS-CoV and SARS-CoV-2 viral products in formalin-fixed paraffin-embedded (FFPE) specimens would be of great utility. A selection of commercial antibodies generated against SARS-CoV spike protein and nucleoprotein, double stranded RNA, and RNA probe for spike genes were evaluated for the ability to detect FFPE infected cells. We also tested both heat- and enzymatic-mediated virus antigen retrieval methods to determine the optimal virus antigen recovery as well as identifying alternative retrieval methods to enable flexibility of IHC methods. In addition to using native virus infected cells as positive control material, the evaluation of non-infected cells expressing coronavirus (SARS, MERS) spike as a biosecure alternative to assays involving live virus was undertaken. Optimized protocols were successfully applied to experimental animal-derived tissues. The diverse techniques for virus detection and control material generation demonstrated in this study can be applied to investigations of coronavirus pathogenesis and therapeutic research in animal models.

A novel coronavirus, SARS-CoV-2, emerged in Central China late 2019, primarily causing a respiratory disease termed COVID-19¹. This virus spread rapidly across the globe and was declared a pandemic by the WHO on the 11th of March 2020. As of October 2020, the pandemic has caused 40 million infections including 1 million deaths globally².

SARS-CoV-2 is a *Betacoronavirus* classified under the order *Nidovirales* and family *Coronaviridae*, with a RNA genome that is closely related to SARS-CoV³. SARS-CoV-2 and SARS-CoV cellular entry is dependent on the receptor angiotensin-converting enzyme 2 (ACE2). Following the activation of spike protein by the cellular priming proteases TMPRSS2 and cathepsins, fusion of viral envelope and cellular membranes occur, allowing the viral genome to enter the host cell⁴. The spike protein, consisting of S1 and S2 subunits, is a major target

¹Pathology Department, Animal and Plant Health Agency (APHA), Woodham Lane, New Haw, Addlestone KT15 3NB, UK. ²Department of Viroscience, Erasmus Medical Centre, Rotterdam, The Netherlands. ³Virology Department, Animal and Plant Health Agency (APHA), Woodham Lane, New Haw, Addlestone KT15 3NB, UK. ⁴Viral Pseudotype Unit, Medway School of Pharmacy, Universities of Greenwich and Kent at Medway, Chatham ME4 4TB, UK. ⁵National Infection Service, Public Health England, Porton Down, Salisbury SP4 0JG, UK. ⁶School of Life Sciences, University of Sussex, Falmer, Brighton BN1 9QG, UK. ⁷Institute for Infection and Immunity, St George's Hospital Medical School, University of London, London SW17 0RE, UK. ✉email: Fabian.lean@apha.gov.uk

Antibody	Species and clonality	Source	Catalogue number	Immunogen	Suitability with antigen retrievals for detection				Optimal dilution	References
					pH 9	pH 6	Proteinase	No retrieval		
Anti-SARS spike	Rabbit mono-clonal	Sino biological	40150-R007	SARS-CoV spike S1 receptor binding domain	Yes	Yes, weaker than pH9	Non-specific	No	1:400–800	Not suitable in earlier report ²⁴
Anti-SARS nucleoprotein	Rabbit mono-clonal	Sino biological	40143-R019	Recombinant SARS-CoV nucleoprotein	Non-specific	Non-specific	Non-specific	n/a	n/a	–
Anti-SARS nucleoprotein	Rabbit poly-clonal	Sino biological	40143-T62	Recombinant SARS-CoV nucleoprotein	Non-specific	Yes	Yes	n/a	1:1000–1500	Used in cell pellet and animal tissues ^{11,24}
Anti-dsRNA [J2]	Rabbit mono-clonal	Absolute antibody	Ab01299-23.0	L-dsRNA	Yes	Yes, weaker than pH9	No	n/a	1:100	–
Anti-dsRNA [J2]	Mouse mono-clonal	Scicons	10010500	L-dsRNA	pH 8	No	No	n/a	1:100	²⁹
Anti-dsRNA [9D5]	Mouse mono-clonal	Absolute antibody	Ab00458-1.1	RDV-RNA-methylated bovine serum albumin complex	No	No	No	n/a	n/a	–
Anti-FIPV	Mouse mono-clonal	Invitrogen	FIPV3-70	FIPV	No	No	No	n/a	1:100	³⁴

Table 1. Antibodies evaluated for immunoreactivity against formalin-fixed paraffin-embedded SARS coronavirus infected cell pellets by immunohistochemistry. *n/a* not applicable, *dsRNA* double stranded RNA, *FIPV* feline infectious peritonitis virus.

for antibody-mediated neutralisation in which immunogenic epitopes reside within the S1 domain^{5,6}. During coronavirus replication, nucleoprotein is the most abundantly expressed proteins, followed by the spike⁷. In addition, during the virus replication cycle, double-stranded RNA (dsRNA) is produced as an intermediate product⁸.

The pathogenicity and transmission dynamics of SARS-CoV-2 differs from SARS-CoV⁹ and there is an urgent requirement to address virological and pathological questions using animal models for human disease and for susceptible animal species. Although not an exhaustive list, experimental investigations have been performed in animal models including ferrets¹⁰, *Cynomolgus* macaques¹¹, Rhesus macaques¹², African green monkeys¹³, Egyptian fruit bats¹⁴, golden Syrian hamsters¹⁵, transgenic hACE2 mice¹⁶, cats^{17,18} and dogs¹⁸. Currently, there are limited reports on the use of immunohistochemistry (IHC) and in situ hybridisation (ISH) targeting virus antigens and genes to define virus-host interactions following in vivo experiments^{11,14} due to a scarcity of suitable reagents and tissues for test development.

Here the suitability of antibodies and RNA probes for the detection of SARS coronaviruses present in formalin-fixed paraffin-embedded (FFPE) specimens using IHC and ISH, respectively, is reported. In addition, options for control materials for test development and quality assurance are described. Subsequently, the comparative utility of these optimised assays on tissues from infected animals and the cellular distribution of virus components is demonstrated.

Results

Detection of SARS-CoV and SARS-CoV-2 antigens. Several commercially available antibodies to SARS-CoV were evaluated using heat (pH6 or 9) and enzymatic-mediated epitope unmasking technique to detect the presence of virus antigens in FFPE native virus infected cell pellets (Table 1). A rabbit monoclonal (mAb; Sino Biological 40150-R007) spike antibody and rabbit polyclonal nucleoprotein antibody (Sino Biological, 40143-T62) were identified to be suitable for IHC on FFPE cell pellets in which specific cytoplasmic chromogen granules were observed in SARS-CoV and SARS-CoV-2 infected cells but not on uninfected cells (Fig. 1a–f). The rabbit monoclonal (mAb; Sino Biological 40150-R007) spike antibody is compatible with either pH9 or 6 retrieval method, whereas rabbit polyclonal nucleoprotein antibody (Sino Biological, 40,143-T62) can be applied on virus antigen retrieved using either heated pH6 buffer or proteinase (Table 1). The detection of nucleoprotein using the same antibody and antigen retrieval method in a different institution (EMC) also demonstrated reproducible immunolabelling (Supp. Figure 1a, b).

Alongside developing the IHC technique to detect SARS-CoV specific antigens, the IHC detection of dsRNA—a viral replicative intermediate was evaluated. Among the three antibodies evaluated, both the J2 recombinant clone raised in mouse and rabbit was able to detect dsRNA in infected cell pellets with cytoplasmic chromogen deposits (Fig. 1g,h; Supp. Figure 1c, d). However, the amount of immunolabelling was not abundant in comparison to SARS specific antigen detection method. The other clone, 9D5, did not generate chromogen deposits with IHC. The cell pellets were also evaluated for non-specific binding using an alphacoronavirus antibody against Feline infectious peritonitis virus (FIPV). No chromogen was detected in uninfected and SARS-CoV infected cells using the FIPV antibody (not shown).

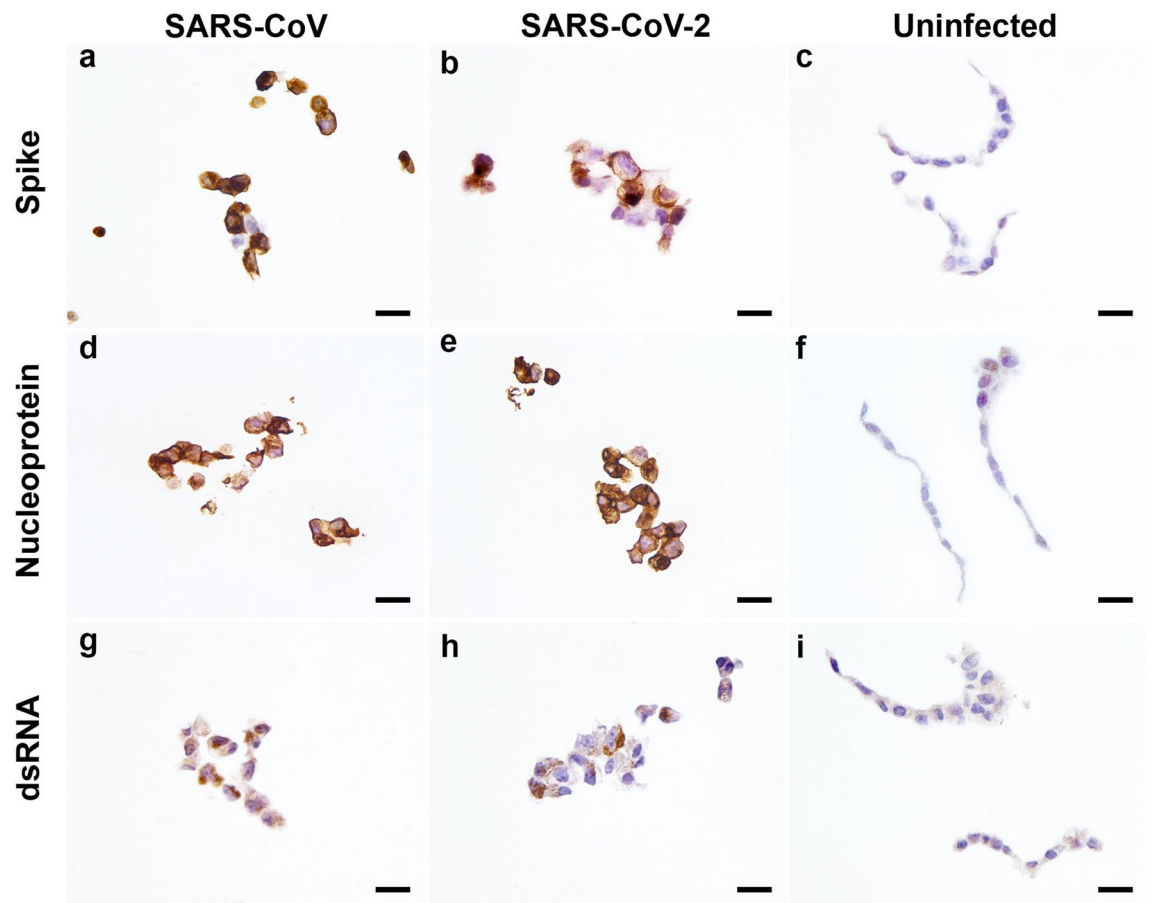


Figure 1. Immunohistochemical labelling of FFPE SARS-CoV and SARS-CoV-2 infected cells and uninfected cells. Immunodetection performed using SARS-CoV spike rabbit monoclonal antibody (a–c), SARS-CoV nucleoprotein rabbit polyclonal antibody (d–f) and double-stranded RNA (dsRNA) rabbit monoclonal antibody (g–i). Scale bars, 20 µm.

Detection of RNA encoding SARS-CoV and SARS-CoV-2 spike protein. One RNAScope® probe was evaluated for the ability to detect SARS coronavirus RNA in FFPE cell pellets. The V-nCoV2019-5 probe did not produce labelling to SARS-CoV (Fig. 2a) but successfully labelled SARS-CoV-2 infected cell pellets (Fig. 2b). Labelling was not observed on uninfected cell pellets (Fig. 2c).

Detection of SARS-CoV and SARS-CoV-2 pseudotype virus in producer cells. To determine if FFPE in vitro generated pseudotype virus expressing recombinant spike protein would be suitable for IHC detection, IHC using the spike mAb identified above was performed on producer cells consisting of lentiviral pseudotype virus expressing either SARS-CoV, SARS-CoV-2 or MERS spike protein. In this assay, the spike mAb was able to detect both SARS-CoV and SARS-CoV-2, displaying specific cytoplasmic and membranous chromogen deposits (Fig. 3a,b). Immunolabelling was not detectable for MERS spike expressing cells (Fig. 3c) or untransfected cells (Fig. 3d).

Application of IHC and ISH on animal tissues. IHC and ISH methods developed and optimised on FFPE cell pellets were tested on nasal turbinates of experimentally derived SARS-CoV-2 infected ferret. Using the spike antibody, immunolabelling was observed specifically labelling the luminal cells in the olfactory epithelial mucosa (Fig. 4a). Nucleoprotein labelling (Fig. 4b) was more ubiquitous in the cytoplasm compared to spike labelling. dsRNA immunolabelling was limited to cytoplasm of the perinuclear region (Fig. 4c), which corresponds to coronavirus replication site¹⁹. As for ISH against spike gene, chromogen was deposited diffusely within the cytoplasm of the infected epithelial cells (Fig. 4d). Serial sections immunolabelled with nucleoprotein, spike or dsRNA antibody (Fig. 4a,c), or spike ISH showed consistent labelling in infected cell population, confirming the specificity of the detection of SARS-CoV-2 in animal tissues.

Discussion

In this report, we described optimized methods for antigen and RNA detection for SARS-CoV and SARS-CoV-2 present in FFPE specimens. Using antibodies raised against SARS-CoV spike and nucleoprotein, we were able to detect the antigens of both SARS-CoV and SARS-CoV-2 present in infected cells and processed for

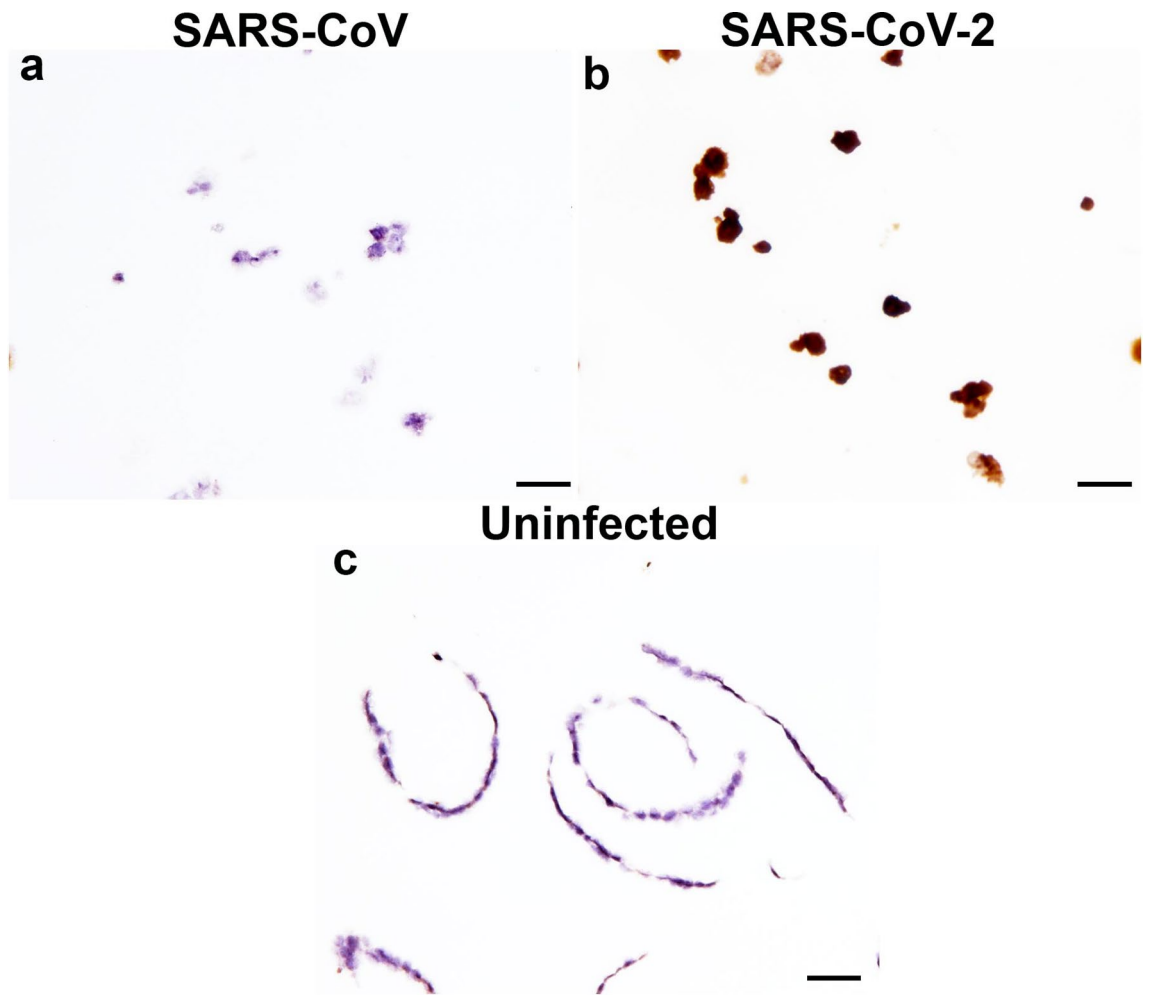


Figure 2. In situ hybridisation (ISH) of FFPE cells infected with SARS-CoV and SARS-CoV-2 using RNAScope[®]. ISH performed using RNA probes designed specific to SARS-CoV-2 spike RNA. SARS-CoV (a) and SARS-CoV-2 infected cells (b), uninfected cells (c). Scale bars, 20 µm.

histology. In addition, RNAScope[®] probe designed specifically for SARS-CoV-2 labelled specifically to cognate virus strain. The detection of a virus replication product, dsRNA, was also evident on IHC. Furthermore, we utilised FFPE pseudotype virus producer cells for SARS-CoV spike IHC and demonstrated the specificity of immunolabelling for both strains of SARS virus.

In IHC or ISH applications, positive control materials are needed to be developed and validated for pathology investigations to ensure the quality of results produced. Susceptible cell lines infected with native virus can be generated for such purpose without a requirement for animal tissues. However, this can be problematic for laboratories that lack high containment facilities required to conduct in vitro work. As an alternative, institutions with the relevant genetic engineering expertise can generate proteins expressed in cell culture through transfection and pseudotype system²⁰, which can be used as an alternative to live virus work to demonstrate the detection of expressed viral proteins following formalin fixation and paraffin embedding.

Although formalin can reliably inactivate infectious agents, fixation can lead to cross-linking of epitopes and impede antibody binding. Enzymatic- or heat-mediated (pH 6 or 9 buffer) antigen retrieval can be applied to re-expose epitopes although the biochemical impact of these methods have not been assessed²¹. Often, only a single antigen-retrieval method, commonly heat-mediated retrieval, is described for the detection of SARS-CoV-2 virus antigen^{22,23}. The spike antibody used in our current study was previously reported as being unsuitable for IHC on FFPE sections²⁴. Here, pH 9 retrieval was demonstrated to be more efficient than pH 6 when attempting to unmask spike epitopes. As for nucleoprotein detection, pH 6 antigen retrieval was reproducible in two separate institutional settings. Further, the suitability of protease antigen retrieval for the detection of nucleoprotein was demonstrated in our study. The versatility of heat- or enzymatic-mediated antigen retrieval for nucleoprotein antigen can provide greater flexibility for investigator to perform multilabelling against other antigen of interest.

As there is growing scientific interest in comparing the pathogenesis of SARS-CoV and SARS-CoV-2, we evaluated the ability of antibodies to cross-react to both virus strains. The spike S1 receptor binding domain (RBD) specific antibody was able to detect spike antigen in both native virus and expressed spike protein of SARS-CoV. Although the RBDs of SARS-CoV and SARS-CoV-2 share only 76% amino acid identity²⁵, the detection with a single preparation of antibody suggests epitope conservation between the two strains assessed. In contrast,

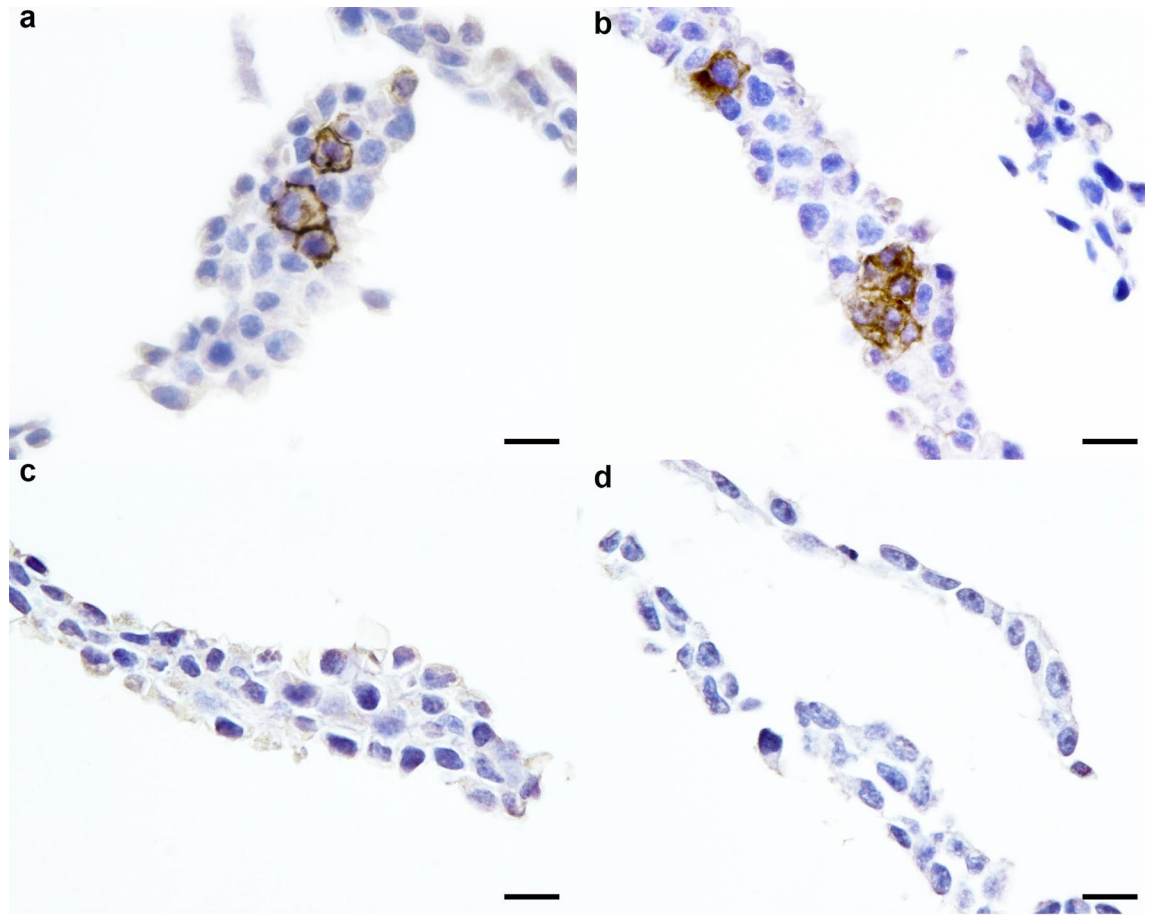


Figure 3. Immunohistochemistry labelling of FFPE cells expressing SARS-CoV, SARS-CoV-2 and MERS spike proteins. Immunodetection performed using SARS-CoV spike rabbit monoclonal antibody on producer cells for SARS-CoV (a), SARS-CoV-2 (b) and MERS-CoV pseudotype virus (c) and non-transfected cells (d). Scale bars, 20 μ m.

the observation that the SARS-CoV spike S1 antibody did not cross react and bind to the MERS spike protein is likely due to the low amino acid homology (33%) between SARS-CoV-2 and MERS-CoV²⁶.

Conversely, the SARS coronavirus nucleoprotein amino acid is highly conserved between SARS-CoV and SARS-CoV-2 with 90% amino acid identity²⁷. This fact was supported by our finding that the nucleoprotein antibody cross-reacted with both viruses. Apart from detecting virus-specific proteins, the virus replicative intermediate dsRNA can also be used to detect RNA viruses including coronaviruses²⁸. In addition to the ability to detect SARS-CoV as described previously²⁸, SARS-CoV-2 can also be detected by IHC using a dsRNA antibody. However, this will require infected cells as positive controls as dsRNA is only synthesised during virus replication.

The utility of these assays was also demonstrated in the detection of viral products in experimentally infected SARS-CoV-2 animal tissues. In the nasal turbinate epithelial cells, dsRNA was present in the peri-nuclear cytoplasm. Early virus replication involves the synthesis of negative-stranded genome template and dsRNA replicative intermediate in which dsRNA was previously observed in the double-membrane vesicles of modified ER membranes situated in the perinuclear region using immunogold staining technique¹⁹. Our study demonstrated spike glycoprotein detection at the apical aspect of respiratory epithelial cells. The localisation was similar to a recent report of SARS-CoV-2 infection of intestinal organoids²⁹.

In conclusion, we have demonstrated the suitability of agarose-embedded infected or transfected cell pellets expressing target proteins, fixed and routinely processed for histopathology, in the development of in situ detection methods for the application in animal model research. This preliminary evaluation of virus detection in histological sections has demonstrated suitability of IHC and ISH on FFPE tissues, and importantly has provided knowledge on the spatial cellular distribution of virus components by conventional light microscopy. The detection of SARS coronavirus antigens and nucleic acids in a cell pellet platform also allowed the rapid development of pathology tools that can be applied in future assessments of SARS-CoV-2 pathogenesis and intervention studies.

Materials and methods

Cells and viruses. Vero E6 cells were maintained in Dulbecco's modified Eagle's medium (DMEM, Gibco) supplemented with 10% foetal calf serum (FCS), HEPES, sodium bicarbonate, penicillin (100 IU/mL) and streptomycin (100 IU/mL). Human embryonic kidney (HEK) 293T-17 cells were grown in DMEM supplemented

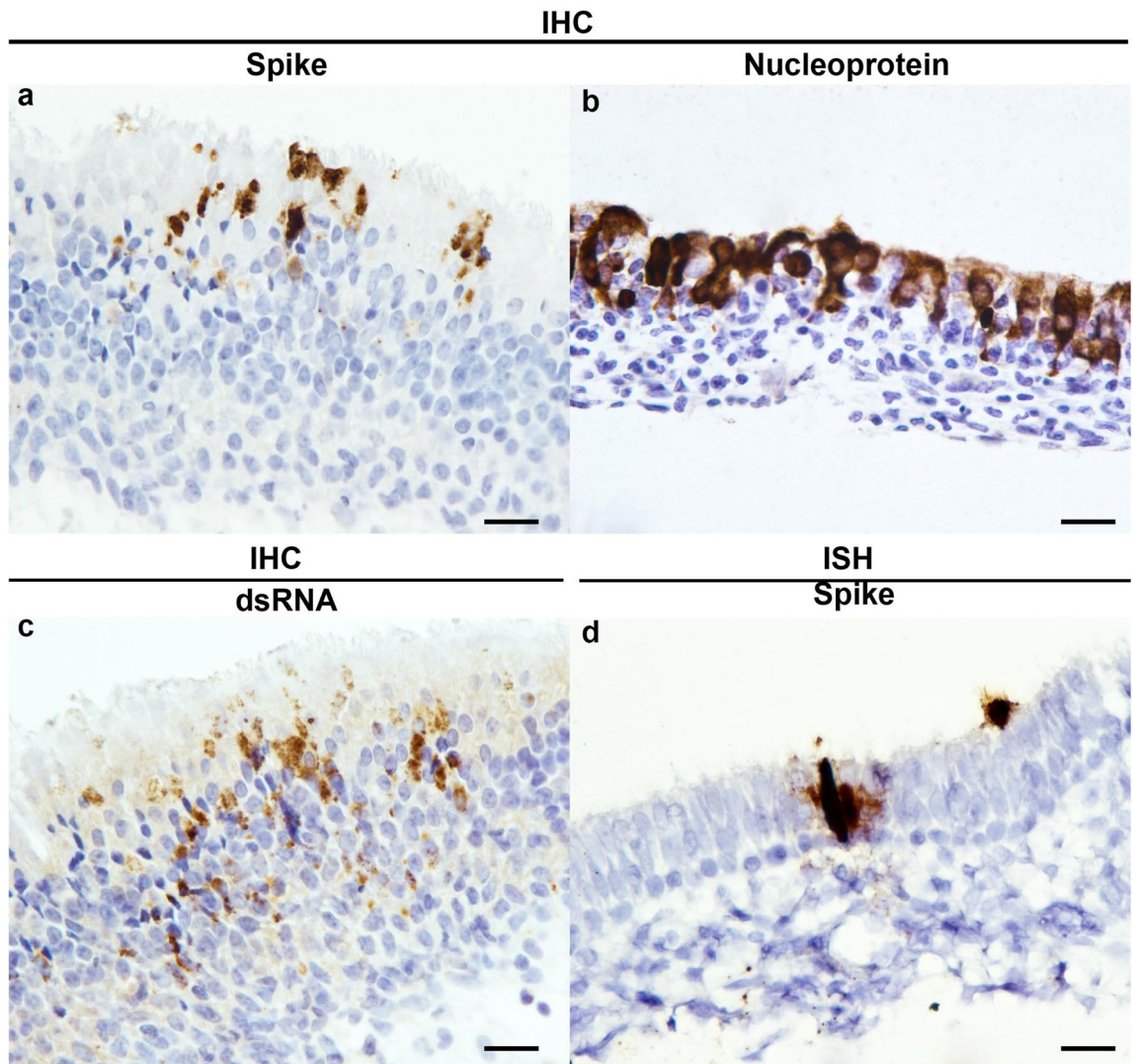


Figure 4. Immunohistochemistry and in situ hybridisation detection of SARS-CoV-2 and RNA on infected ferret tissues. Detection of spike protein (a), nucleoprotein (b) and dsRNA antigens (c) and spike RNA (d) labelling. Tissue shrinkage artefact with ISH pre-treatment (d). Scale bars, 20 μ m.

with FCS, penicillin (100 IU/mL) and streptomycin (100 IU/mL). Cells were grown at 37 °C in a humidified CO₂ incubator. SARS-CoV (isolate HKU-39849)²⁹ and SARS-CoV-2 (isolate BetaCoV/Munich/BavPat1/2020; European Virus Archive Global #026V-03883)²⁹ were used for in vitro work whilst SARS-CoV-2 (nCoV/Victoria/1/2020) was used for in vivo experimentation³⁰. Both SARS-CoV and SARS-CoV-2 were propagated on VeroE6 (ATCC® CRL 1586TM) cells in Opti-MEM I (1X) + GlutaMAX (ThermoFisher), supplemented with penicillin (100 IU/mL) and streptomycin (100 IU/mL) at 37 °C in a humidified CO₂ incubator. Stocks were produced by infecting VeroE6 cells at a multiplicity of infection (MOI) of 0.01 and incubating the cells for 72 h (hours). The culture supernatant was cleared by centrifugation and stored in aliquots at -80 °C. Investigations using infectious virus were performed within the biosafety level 3 laboratory at the Erasmus Medical Centre (EMC), Netherlands.

Generation of virus infected cells. Vero E6 cells were inoculated with SARS-CoV and SARS-CoV-2 at a MOI of 0.3. After 24 h post-infection, cells were fixed with 10% neutral buffer formalin (NBF) along with a separate flask of non-infected cells.

Generation of virus pseudoparticle in producer cells. Recombinant spike protein was pseudotyped onto a lentiviral core as previously described^{31,32}. This was conducted in a BSL2 laboratory in APHA. Briefly, HEK 293T-17 cells were transfected with p8.91 (gag-pol), pCAGGS-s (full length SARS-CoV, SARS-CoV-2, or MERS spike), and pCSFLW. At 5 days post-transfection, cells were fixed with 10% NBF.

Preparation of cells for histology processing. Fixed monolayer of cells from in vitro infection or transfection were scraped off flasks and centrifuged at 1500 g. Following removal of supernatant, cell pellets were

re-suspended in 2% agarose (Sigma) and allowed to set. Agarose-embedded cell pellets were then processed by routine histology method on a histology processor³³.

Animal experimental infection. In vivo experimentations were undertaken within the Advisory Committee on Dangerous Pathogens level 3 (ACDP3) certified animal complex of APHA, UK, in accordance to the Animal (Scientific Procedures) Act 1986. The animal experiment was approved by APHA Animal Welfare and Ethical Review Body (AWERB; HOL-PP3405816/1/001). Ferrets were inoculated intranasally with 1 ml of SARS-CoV-2 of 2×10^6 tissue culture infectious dose 50 (TCID₅₀). Animals were humanely euthanised at pre-determined time-points and tissues collected into 10% NBF.

Immunohistochemistry (IHC). Four micrometre thick sections were dewaxed and rehydrated through xylene and graded alcohol, respectively, quenched for endogenous peroxidase with 3% hydrogen peroxide in methanol (VWR International) for 15 min (minutes) at room temperature (RT), before epitope unmasking using pH6 (10 mM citric acid buffer, adjusted to pH6 with 1 M sodium hydroxide; Fisherscientific), pH9 target retrieval buffer (Envision FLEX, high pH; Dako) for 10 min at 97 °C, or proteinase XXIV (Sigma-Aldrich) for 15 min at RT. Slides were blocked with normal goat serum for 30 min in RT (1/66 dilution; Vector Laboratories) and assembled into cover plates to facilitate IHC using the Shandon Sequenza system (Shandon). Samples were then incubated with a primary antibody at 4 °C overnight or 1 h at RT, followed by incubation with mouse- or rabbit-specific Envision™ polymer (Dako) for 30 min at RT and visualised using 3,3-diaminobenzidine (DAB) (Sigma Aldrich) for 10 min at RT. Tris-buffered saline with Tween (145 mM NaCl, 5 mM Tris(hydroxymethyl) methylamine, 0.1% w/v Tween*20, adjusted to pH7.6 with 1 M HCl; Fisher Scientific; VWR International) were used for rinsing sections between incubations. Subsequently, sections were counterstained in Mayer's haematoxylin (Surgipath), dehydrated in ethanol and xylene, and glass coverslips mounted using Dibutyl Phthalate Xylene.

In situ hybridisation (ISH). Twenty pairs of double Z proprietary RNA probes targeting the spike gene of SARS-CoV-2, (V-nCoV2019-5, catalogue no. 848569) were synthesised by Advanced Cell Diagnostics (ACD, USA). ISH was performed using the RNAScope® 2.5 HD Brown Detection Kit (ACD) as per manufacturer's instructions. Tissues were dewaxed and hydrated through xylene and alcohol, respectively, treated with RNAScope® hydrogen peroxide (ACD) for 10 min at RT, and heat-mediated retrieval using Target Retrieval Solution (ACD) for 18 min at 97 °C and Protease Plus (ACD) for 10 min at 40 °C. RNA probes were then added to sections to allow hybridisation for 2 h at 40 °C and followed by 6 rounds of amplification with Hybridise Amp (ACD) at 40 °C, alternating between 30 and 15 min incubation, in the HyBEZ™ oven (ACD). Slides were washed with 1× wash buffer (ACD) for 2 min at RT between incubations. Signal was detected using DAB. Sections were counter-stained with Mayer's haematoxylin (Surgipath), dehydrated in ethanol and xylene, and glass coverslips mounted with Cytoseal (ACD).

Data availability

All data generated or analysed during this study are included in this published article (and its Supplementary Information files).

Received: 16 July 2020; Accepted: 25 November 2020

Published online: 14 December 2020

References

- Zhu, N. *et al.* A novel coronavirus from patients with pneumonia in China, 2019. *N. Engl. J. Med.* **382**, 727–733. <https://doi.org/10.1056/NEJMoa2001017> (2020).
- JHU. *COVID-10 Dashboard*, <https://coronavirus.jhu.edu/map.html> (2020).
- Coronaviridae Study Group of the International Committee on Taxonomy of V. The species severe acute respiratory syndrome-related coronavirus: Classifying 2019-nCoV and naming it SARS-CoV-2. *Nat. Microbiol.* **5**, 536–544. <https://doi.org/10.1038/s41564-020-0695-z> (2020).
- Hoffmann, M. *et al.* SARS-CoV-2 cell entry depends on ACE2 and TMPRSS2 and is blocked by a clinically proven protease inhibitor. *Cell* **181**, 271–280 e278. <https://doi.org/10.1016/j.cell.2020.02.052> (2020).
- He, Y., Li, J., Heck, S., Lustigman, S. & Jiang, S. Antigenic and immunogenic characterization of recombinant baculovirus-expressed severe acute respiratory syndrome coronavirus spike protein: Implication for vaccine design. *J. Virol.* **80**, 5757–5767. <https://doi.org/10.1128/JVI.00083-06> (2006).
- Lan, J. *et al.* Structure of the SARS-CoV-2 spike receptor-binding domain bound to the ACE2 receptor. *Nature* **581**, 215–220. <https://doi.org/10.1038/s41586-020-2180-5> (2020).
- Irigoyen, N. *et al.* High-resolution analysis of coronavirus gene expression by RNA sequencing and ribosome profiling. *PLoS Pathog.* **12**, e1005473. <https://doi.org/10.1371/journal.ppat.1005473> (2016).
- Ivanov, K. A. *et al.* Multiple enzymatic activities associated with severe acute respiratory syndrome coronavirus helicase. *J. Virol.* **78**, 5619–5632. <https://doi.org/10.1128/JVI.78.11.5619-5632.2004> (2004).
- Peiris, J. S., Yuen, K. Y., Osterhaus, A. D. & Stohr, K. The severe acute respiratory syndrome. *N. Engl. J. Med.* **349**, 2431–2441. <https://doi.org/10.1056/NEJMra032498> (2003).
- Kim, Y. I. *et al.* Infection and rapid transmission of SARS-CoV-2 in ferrets. *Cell Host Microbe* **27**, 704–709 e702. <https://doi.org/10.1016/j.chom.2020.03.023> (2020).
- Rockx, B. *et al.* Comparative pathogenesis of COVID-19, MERS, and SARS in a nonhuman primate model. *Science* **368**, 1012–1015. <https://doi.org/10.1126/science.abb7314> (2020).
- Munster, V. J. *et al.* Respiratory disease in rhesus macaques inoculated with SARS-CoV-2. *Nature* <https://doi.org/10.1038/s41586-020-2324-7> (2020).
- Woolsey, C. *et al.* Establishment of an African green monkey model for COVID-19. *bioRxiv* <https://doi.org/10.1101/2020.05.17.100289> (2020).

14. Schlottau, K. *et al.* SARS-CoV-2 in fruit bats, ferrets, pigs, and chickens: An experimental transmission study. *Lancet Microbe* **1**, e218–e225. [https://doi.org/10.1016/s2666-5247\(20\)30089-6](https://doi.org/10.1016/s2666-5247(20)30089-6) (2020).
15. Chan, J. F. *et al.* Simulation of the clinical and pathological manifestations of coronavirus disease 2019 (COVID-19) in golden Syrian hamster model: Implications for disease pathogenesis and transmissibility. *Clin. Infect. Dis.* <https://doi.org/10.1093/cid/ciaa325> (2020).
16. Bao, L. *et al.* The pathogenicity of SARS-CoV-2 in hACE2 transgenic mice. *Nature* <https://doi.org/10.1038/s41586-020-2312-y> (2020).
17. Shi, J. *et al.* Susceptibility of ferrets, cats, dogs, and other domesticated animals to SARS-coronavirus 2. *Science* (2020).
18. Bosco-Lauth, A. M. *et al.* Experimental infection of domestic dogs and cats with SARS-CoV-2: Pathogenesis, transmission, and response to reexposure in cats. *Proc. Natl. Acad. Sci.* **117**, 26382–26388. <https://doi.org/10.1073/pnas.2013102117> (2020).
19. Knoops, K. *et al.* SARS-coronavirus replication is supported by a reticulovesicular network of modified endoplasmic reticulum. *PLoS Biol.* **6**, e226. <https://doi.org/10.1371/journal.pbio.0060226> (2008).
20. Nicholls, J. M. *et al.* Time course and cellular localization of SARS-CoV nucleoprotein and RNA in lungs from fatal cases of SARS. *PLoS Med.* **3**, e27. <https://doi.org/10.1371/journal.pmed.0030027> (2006).
21. Ramos-Vara, J. A. & Miller, M. A. When tissue antigens and antibodies get along: Revisiting the technical aspects of immunohistochemistry—The red, brown, and blue technique. *Vet. Pathol.* **51**, 42–87. <https://doi.org/10.1177/0300985813505879> (2014).
22. Best Rocha, A. *et al.* Detection of SARS-CoV-2 in formalin-fixed paraffin-embedded tissue sections using commercially available reagents. *Lab. Invest.* <https://doi.org/10.1038/s41374-020-0464-x> (2020).
23. Carossino, M. *et al.* Detection of SARS-CoV-2 by RNAscope® in situ hybridization and immunohistochemistry techniques. *Adv. Virol.* **165**, 2373–2377. <https://doi.org/10.1007/s00705-020-04737-w> (2020).
24. Liu, J. *et al.* Molecular detection of SARS-CoV-2 in formalin-fixed, paraffin-embedded specimens. *JCI Insight* **5**, <https://doi.org/10.1172/jci.insight.139042> (2020).
25. Wan, Y., Shang, J., Graham, R., Baric, R. S. & Li, F. Receptor recognition by the novel coronavirus from Wuhan: An analysis based on decade-long structural studies of SARS coronavirus. *J. Virol.* **94**, <https://doi.org/10.1128/JVI.00127-20> (2020).
26. Okba, N. M. A. *et al.* Severe acute respiratory syndrome coronavirus 2-specific antibody responses in coronavirus disease patients. *Emerg. Infect. Dis.* **26**, 1478–1488. <https://doi.org/10.3201/eid2607.200841> (2020).
27. Zhou, P. *et al.* A pneumonia outbreak associated with a new coronavirus of probable bat origin. *Nature* **579**, 270–273. <https://doi.org/10.1038/s41586-020-2012-7> (2020).
28. Richardson, S. J. *et al.* Use of antisera directed against dsRNA to detect viral infections in formalin-fixed paraffin-embedded tissue. *J. Clin. Virol.* (2010).
29. Lamers, M. M. *et al.* SARS-CoV-2 productively infects human gut enterocytes. *Science* **369**, 50–54. <https://doi.org/10.1126/science.abc1669> (2020).
30. Caly, L. *et al.* Isolation and rapid sharing of the 2019 novel coronavirus (SARS-CoV-2) from the first patient diagnosed with COVID-19 in Australia. *Med. J. Aust.* <https://doi.org/10.5694/mja2.50569> (2020).
31. Grehan, K., Ferrara, F. & Temperton, N. An optimised method for the production of MERS-CoV spike expressing viral pseudotypes. *MethodsX* **2**, 379–384. <https://doi.org/10.1016/j.mex.2015.09.003> (2015).
32. Thompson, C. *et al.* Neutralising antibodies to SARS coronavirus 2 in Scottish blood donors—A pilot study of the value of serology to determine population exposure. medRxiv:2020.2004.2013.20060467, <https://doi.org/10.1101/2020.04.13.20060467> (2020).
33. Puranik, A. *et al.* Transmission dynamics between infected waterfowl and terrestrial poultry: Differences between the transmission and tropism of H5N8 highly pathogenic avian influenza virus (clade 2.3.4.4a) among ducks, chickens and turkeys. *Virology* **541**, 113–123 (2020).
34. Garner, M. M. *et al.* Clinicopathologic features of a systemic coronavirus-associated disease resembling feline infectious peritonitis in the domestic ferret (*Mustela putorius*). *Vet. Pathol.* **45**, 236–246. <https://doi.org/10.1354/vp.45-2-236> (2008).

Acknowledgements

SARS-CoV HKU-39849 and SARS-CoV-2 BetaCoV/Munich/BavPat1/2020 virus isolates were kindly provided by Professor Malik Peiris, University of Hong Kong and Professor Christian Drosten, Charité Universitätsmedizin, respectively. We also appreciate Victorian Infectious Diseases Reference Laboratory (VIDRL) and the Peter Doherty Institute, Australia (Dr Julian Druce) for sharing the virus isolate nCoV/Victoria/2/2020. We would like to thank staff at the histology laboratory at APHA. The study was funded by Department for Environment, Food & Rural Affairs (DEFRA), UK (Project SE0557, EXOM0414, SV3700). Funder has no role in study design, analysis, interpretation or writing of the report.

Author contributions

F.Z.X.L., M.M.L., R.S. and S.P.S. performed the experiments. F.Z.X.L., M.M.L. and A.N. conducted formal analysis. F.Z.X.L., M.M.L., D.S., N.T. and K.R.B. provided the methodology. I.B., S.M.B., M.W.C., B.L.H., A.C.B. and A.N. provided with resources. F.Z.X.L. and M.M.L. wrote the original draft. All authors (F.Z.X.L., M.M.L., S.P.S., R.S., D.S., N.T., B.L.H., A.C.B., K.R.B., M.W.C., S.M.B., I.B. and A.N.) reviewed and edited the manuscript.

Competing interests

The authors declare no competing interests.

Additional information

Supplementary Information The online version contains supplementary material available at <https://doi.org/10.1038/s41598-020-78949-0>.

Correspondence and requests for materials should be addressed to F.Z.X.L.

Reprints and permissions information is available at www.nature.com/reprints.

Publisher's note Springer Nature remains neutral with regard to jurisdictional claims in published maps and institutional affiliations.



Open Access This article is licensed under a Creative Commons Attribution 4.0 International License, which permits use, sharing, adaptation, distribution and reproduction in any medium or format, as long as you give appropriate credit to the original author(s) and the source, provide a link to the Creative Commons licence, and indicate if changes were made. The images or other third party material in this article are included in the article's Creative Commons licence, unless indicated otherwise in a credit line to the material. If material is not included in the article's Creative Commons licence and your intended use is not permitted by statutory regulation or exceeds the permitted use, you will need to obtain permission directly from the copyright holder. To view a copy of this licence, visit <http://creativecommons.org/licenses/by/4.0/>.

© The Author(s) 2020